

Joint Backhaul-Access Analysis of Full Duplex Self-Backhauling Heterogeneous Networks

Ankit Sharma, Radha Krishna Ganti and J. Klutto Milleth

Abstract

With the successful demonstration of in-band full-duplex (IBFD) transceivers, a new research dimension has been added to wireless networks. This paper proposes a use case of this capability for IBFD self-backhauling heterogeneous networks (HetNet). IBFD self-backhauling in a HetNet refers to IBFD-enabled small cells backhauling themselves with macro cells over the wireless channel. Owing to their IBFD capability, the small cells simultaneously communicate over the access and backhaul links, using the same frequency band. The idea is doubly advantageous, as it obviates the need for fiber backhauling small cells every hundred meters and allows the access spectrum to be reused for backhauling at no extra cost. This work considers the case of a two-tier cellular network with IBFD-enabled small cells, wirelessly backhauling themselves with conventional macro cells. For clear exposition, the case considered is that of FDD network, where within access and backhaul links, the downlink (DL) and uplink (UL) are frequency duplexed (f_1 , f_2 respectively), while the total frequency spectrum used at access and backhaul ($f_1 + f_2$) is the same. Analytical expressions for coverage and average downlink (DL) rate in such a network are derived using tools from the field of *stochastic geometry*. It is shown that DL rate in such networks could be close to double that of a conventional TDD/FDD self-backhauling network, at the expense of reduced coverage due to higher interference in IBFD networks. For the proposed IBFD network, the conflicting aspects of increased interference on one side and high spectral efficiency on the other are captured into a mathematical model. The mathematical model introduces an end-to-end joint analysis of backhaul (or fronthaul) and access links, in contrast to the largely available access-centric studies. .

Ankit Sharma and Radha Krishna Ganti were with the Electrical Engineering Department at Indian Institute of Technology, Madras at the time of submission. Their contact emails are {ankitsharma, rganti}@ee.iitm.ac.in. Ankit Sharma is now with Cypress Semiconductors India Pvt. Ltd. (ansa@cypress.com). J. Klutto Milleth is with Center of Excellence in Wireless Technology, IIT-Madras Research Park. His contact email is klutto@cewit.org.in

I. INTRODUCTION

Capacity demands in a wireless cellular system have been increasing at a rapid pace. The next move towards 5G network aims at increasing capacity of the current systems thousand fold [1]. Since bandwidth demands have ever been exceeding the available spectrum, frequency reuse techniques are becoming increasingly important for cellular systems. The well studied dense heterogeneous network (HetNet) [2] is one of the methods to increase capacity for future networks. Typically, HetNet consists of a macro base-station (M-BS) tier, serving high mobility users overlaid with operator deployed pico base-station (P-BS) tier (a.k.a. small cells) [3] for low mobility, dense user areas. Deploying a highly dense network of P-BSs is becoming increasingly worrisome [4] for operators. This is because fiber backhauling such P-BSs placed every few tens of meters is not a practically and economically viable option, especially in developing countries like India. The alternative is to employ wireless backhauling. Though wireless backhauling obviates the need for laying down high-speed/fiber links, it needs the operator to partition their highly priced spectrum into orthogonal access and backhauling resources, thereby resulting in lower spectral usage for user access.

In-band full-duplex (IBFD) systems—another frequency reuse technique—present a scheme to wirelessly backhaul P-BSs with M-BSs without having to orthogonalize allocated spectrum between access and backhaul. The scheme consists of a two-tier cellular network where the P-BSs, being IBFD-enabled, backhaul themselves wirelessly with the M-BSs, which themselves are fiber-backhauled to the core network. The M-BSs exchange backhaul data with the P-BSs on the entire spectrum that the P-BSs use to transmit data to the users. M-BSs may also serve the users directly. Since practical IBFD radio systems ([5], [6], [7] and [8]) have already been demonstrated, the proposed scheme results in an amalgamation of two frequency reuse techniques working in tandem. To this end, the paper analyzes and gives key design insights for a future cellular network¹ that leverages the efficiency of IBFD radios used in a wirelessly backhauled two-tier HetNet.

¹Since the paper studies a two-tier HetNet architecture based on each tier being FDD in its own uplink and downlink, comparison of IBFD-enabled networks will be done with the conventional FDD systems (with no IBFD-enabled station) throughout the paper.

A. Related Work

For a self-backhauled two-tier HetNet, a model for joint analysis of backhaul-access links is required, which is a rather less studied topic. The topic finds mention in [9], where it is listed as one of the potential applications of IBFD radios. Work in [10] is an attempt in this direction, though the work develops on the basic assumption of one P-BS per user and inter P-BS interference has not been considered. Moreover, the paper only presents capacity results as a function of physical separation between the P-BS and M-BS while the overall coverage trends in such a two-tier network have not been analyzed. Perhaps a closely related work in this direction is found in [11], where the authors model a multiple-input-multiple-output (MIMO) IBFD P-BS and conventional half-duplex (HD) backhauling M-BS. The M-BSs only play the role of backhaul aggregators and do not provide access communication to users. The probability of successful transmissions is modeled as a product of independent successful transmissions for first hop (M-BS to P-BS) and second hop (P-BS to user) in the downlink (DL). This might not be always true of real systems where there might be dependence between the two probabilities. Also, the aggregate rate characterization from the M-BS to the user has not been detailed.

Other works like [12] analyze an IBFD network for parameters like rate but only for a single-tier network. They allocate same channels to both uplink (UL) and DL of base station-to-user link and compute the parameters thereof. Work in [13] discusses the optimal power allocation strategy in IBFD networks using relays. The work builds on a cognitive setup with primary and secondary nodes in general. Interference is then controlled from primary transmitters to secondary receivers. The approach is modeled as an optimization problem for transmit powers of primary and secondary transmitters. Works in [14] and [15] discuss about bringing in MIMO and beamforming on IBFD radios and the benefits thereof, though [14] uses only a single tier. Two interesting analyses are offered through works in [16] and [17] where the authors argue the use of IBFD at all. The authors pitch the use case of using multiple antennas for the conventional HD multiple-input-multiple-output (MIMO) operation versus using the antennas for IBFD operation. In fact, most of the cases discuss only the access link optimization. Another relevant study in self-backhauling is the recent work in [18]. The authors present the system level coverage and rate results in a mesh network of base-stations (BS) with wired backhaul, providing wireless backhauling for BSs without wired backhaul. However, the study is done for millimeter-wave networks without IBFD capability. Previous work on similar HetNet architecture was presented

in [19], but was limited to a single path loss exponent being used for both the P-BS as well as the M-BS tier. This work generalizes [19] to two different path loss exponents which is practically more relevant.

B. Our approach and novelty

The paper proposes a two-tier network consisting of IBFD-enabled P-BSs and conventional M-BSs. It analyzes the performance of the system in the DL. The setup consists of P-BSs being wirelessly backhauled by the M-BSs. Since the P-BSs are IBFD-enabled, they use the same set of frequencies to backhaul themselves on the DL and UL with the M-BS, as the ones they use in the DL and UL access links to the users (say, f_1 and f_2 be the DL and UL frequency for the P-BS to user (and M-BS to P-BS in backhaul) link and user to P-BS (and P-BS to M-BS in backhaul) link transmissions). The M-BSs being conventional non-IBFD stations, need to bifurcate frequency resources between backhaul and access links. For 1 Hz of bandwidth, the M-BSs use η Hz ($0 \leq \eta \leq 1$) for backhauling and $(1 - \eta)$ Hz for direct access links to users. It is interesting to note that the design fits *as-is* for a frequency division duplexed IBFD network and could be tailored to suit other networks, such as TDD as well. Moreover, the design requires only the P-BSs to be IBFD, while the user devices and M-BS could work on legacy FDD mode (refer Fig. 1a).

For the given two-tier network, Poisson Point Process (PPP) ([20] and [21]) is used for the spatial distribution of nodes (P-BS and M-BS). The main contributions of this work are listed below:

- A novel HetNet architecture, leveraging IBFD capability is proposed and the coverage probability and average rate for a typical user in such a network are derived.
- The paper achieves mathematical derivation of the exact coverage and rate parameters for the proposed IBFD HetNet. Though it is intuitive to see that spectrum reuse increases rates at the expense of decreased coverage due to wireless backhaul links, an exact quantification of these two contrasting effects has been established in this work. Tractable and quickly computable coverage expressions are important for system analysis of future IBFD-enabled HetNets. The analysis also identifies inter-tier interference and the bandwidth division at the backhauling M-BS as the main limiting factors in such HetNets.
- In the proposed network, the effective signal-to-interference (SIR) ratio distribution for a

typical user associated with a P-BS is modeled as the joint SIR distribution of the {user-P-BS, P-BS-M-BS} link-pair. Therefore the coverage under P-BS implies joint coverage – of the typical user under a P-BS, along with coverage of the same P-BS with a backhauling M-BS. The average rate for a P-BS associated user is modeled as the minimum of rates on the {user-P-BS, P-BS-M-BS} link-pair. This introduces inter-dependence between the two tiers.

In [22], the coverage probability was obtained in a general K-tier HetNet, but without any dependence between the tiers themselves. In the proposed network, since the backhaul links are also active over the wireless channel, interference to access links of users is enhanced and the coverage degrades. On the other hand, reusing the access spectrum for wireless backhauling in an IBFD setting tends to double the spectral efficiency of the system. This work models and details the way these two contrasting factors affect the overall system behavior.

II. SYSTEM MODEL

The system model considered in this paper is described in the following sub-sections.

A. Spatial arrangement of base-stations

The location of the M-BSs and P-BSs are assumed to follow independent Poisson point processes $\Phi_m \subset \mathbb{R}^2$ and $\Phi_s \subset \mathbb{R}^2$ with densities λ_m and λ_s , respectively. The transmit powers of the M-BS and P-BS tier are assumed to be P_m and P_s respectively. Small scale fading between any pair of nodes is assumed to be independent and Rayleigh distributed. The fading power (square of the small scale fading) between nodes located at points x and y in \mathbb{R}^2 is denoted by g_{xy} and is exponentially distributed, also with unit mean. Basic large scale path loss function is used, i.e., the power received at distance r when transmitting at unity power is given as $r^{-\alpha}$, where $\alpha > 2$ is the path loss exponent. Path loss exponents for M-BS and P-BS tiers are denoted by α_m and α_s , respectively. Without loss of generality, a typical user located at the origin is considered and the performance of this typical user in the DL is analyzed.

B. Association Model

The association rule is based on the maximum average received biased power as discussed in [23]. Biasing a user to associate with a P-BS even if the received power from a M-BS is higher,

helps offload traffic from the M-BSs. Hence, for BS association, the average received biased power at the typical user is $P_s B_s \|x_s\|^{-\alpha_s}$ and $P_m B_m \|x_m\|^{-\alpha_m}$ for P-BS and M-BS respectively, where B_s and B_m , and x_s and x_m represent their respective biases and distances from the typical user at the origin. Let $x_{s,min}$ and $x_{m,min}$ denote the distance of the closest P-BS and M-BS respectively, to the user at the origin. Then the user connects to the P-BS if $x_{m,min} \geq \Delta_m^{-1} x_{s,min}^{\alpha_s/\alpha_m}$ and to the closest M-BS, otherwise. Here $\Delta_m = ((P_s B_s)/(P_m B_m))^{1/\alpha_m}$. Let ε_m and ε_s denote the events of M-BS and P-BS association respectively, of the typical user. Then the corresponding probabilities of association are given in [23] as,

$$\Pr(\varepsilon_s) = 2\pi\lambda_s \int_0^\infty e^{-\pi\left(\lambda_m \Delta_m^{-2} x_{s,min}^{\frac{2\alpha_s}{\alpha_m}} + \lambda_s x_{s,min}^2\right)} x_{s,min} dx_{s,min} ; \quad \Pr(\varepsilon_m) = 1 - \Pr(\varepsilon_s). \quad (1)$$

C. Bandwidth Allocation

Bandwidth allocation between the P-BS and M-BS tiers is discussed next, considering $2W$ Hz of allocated spectrum.

Full-Duplex Bandwidth Allocation: For IBFD networks, the available spectrum of $2W$ Hz is allocated as:

- 1) The entire $2W$ Hz is used by P-BSs and M-BSs.
- 2) Within each tier, $2W$ Hz is divided into UL and DL resources utilizing W Hz each (as for conventional FDD).
- 3) At the M-BSs (being non-IBFD), W Hz is further sub-divided as ηW Hz and $(1 - \eta)W$ Hz, $0 \leq \eta \leq 1$, for backhaul and access resources respectively.
- 4) Also, each M-BS to P-BS link is limited in bandwidth to $\left(\frac{\eta}{n}\right) W$ Hz, considering each M-BS backhauled $n = \lambda_s/\lambda_m$ P-BSs on an average.

Half-Duplex Bandwidth Allocation: For conventional FDD networks, the available $2W$ Hz is allocated as:

- 1) $\kappa 2W$ Hz and $(1 - \kappa)(2W)$ Hz, $0 \leq \kappa < 1$, partitioned between M-BSs and P-BSs respectively. Typically, $\kappa = 0.5$, so each tier gets W Hz. Notice that this is in contrast to both the tiers getting the entire $2W$ Hz in IBFD case.
- 2) At each tier, W Hz is divided into UL and DL resources utilizing $W/2$ Hz each.
- 3) At the M-BSs, $W/2$ Hz is further sub-divided as $\eta W/2$ Hz and $(1 - \eta)W/2$ Hz, $0 \leq \eta \leq 1$, for backhauling and access resources respectively.

- 4) Also, each M-BS to P-BS link is limited in bandwidth to $\left(\frac{n}{n}\right) W/2$ Hz, considering each M-BS backhauls $n = \lambda_s/\lambda_m$ P-BSs on an average.

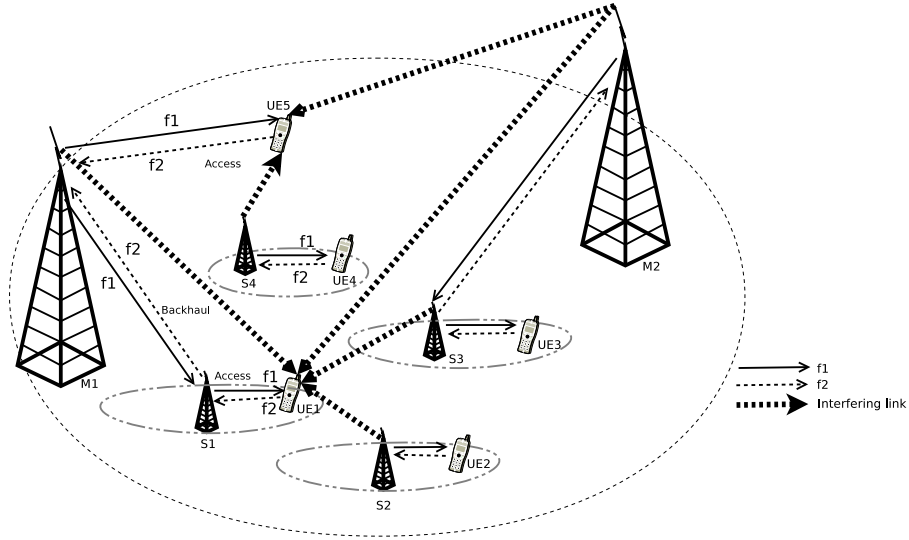


Fig. 1a: DL interference in IBFD system. Total spectrum = $2W$ Hz. Each link represents a bandwidth of W Hz. For instance, the DL backhaul link is centered around f_1 Hz and has a bandwidth of W Hz. Users attached to either P-BS or M-BS receive interference from both the tiers. The given spectrum though, is entirely used by both the tiers.

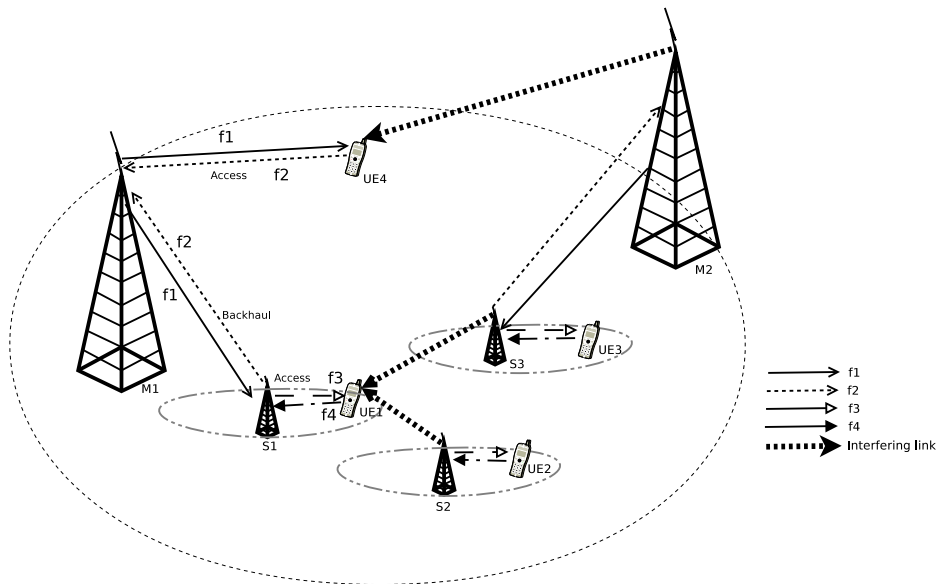


Fig. 1b: DL interference in conventional FDD system. Total spectrum = $2W$ Hz. Each link represents a bandwidth of $W/2$ Hz. For instance, the DL backhaul link is centered around f_1 Hz and has a bandwidth of $W/2$ Hz. Users attached to a tier (P-BS or M-BS) receive interference from only from that tier. However, the given spectrum needs to be partitioned between the tiers.

Taking the case of an IBFD system, the proposed frequency allocation plan is depicted in Fig. 1a. For conventional FDD system the frequency plan is well known and depicted in Fig. 1b. The figures denote DL and UL carriers as $f1$ and $f2$ respectively, that are centered about the bandwidth of W Hz and $W/2$ Hz in IBFD and conventional FDD case respectively. In IBFD systems, both P-BSs and M-BSs use the total available spectrum but interference is more, as shown by the thick broken lines in Fig. 1a. For conventional FDD systems, though the interferers are only the nodes belonging to the tier to which the user is associated, the total available spectrum is partitioned between the M-BS and P-BS.

D. Signal-to-Interference Ratio

An interference limited network is assumed and signal-to-interference-plus-noise ratio (SINR) is replaced SIR [22] as the measure of performance.

1) *Small cell association*: Consider a typical user at the origin associated with a P-BS. Let point $r_s \in \Phi_s$ denote this closest P-BS to the typical user. Let the point $r_m \in \Phi_m$ denote the closest M-BS to the aforementioned P-BS. The P-BS associates with the closest M-BS for backhaul. Let SIR_{us} denote SIR of the signal from the P-BS to the user in DL access. Then

$$\text{SIR}_{us}(r_s, r_m) = \frac{P_s g_{or_s} \|r_s\|^{-\alpha_s}}{I_s(o) + I_m(o) + P_m g_{or_m} \|r_m\|^{-\alpha_m}} \quad (2)$$

where,

$$I_s(x) = \sum_{z \in \Phi_s \cap B(o, r_s)^c} P_s g_{xz} \|z - x\|^{-\alpha_s},$$

is the interference from other P-BSs to a user located at a point x in \mathbb{R}^2 and $B(o, r_s)$ denotes a disc centered at origin o , having radius r_s and $B(o, r_s)^c$ denotes its complement. The interference from the M-BS to a user located at a point x in \mathbb{R}^2 is

$$I_m(x) = \sum_{z \in \Phi_m \cap \mathcal{M}} P_m g_{xz} \|z - x\|^{-\alpha_m},$$

where $\mathcal{M} = (B(o, r_s^{\alpha_s/\alpha_m} \Delta_m^{-1}) \cup B(r_s, \|r_m - r_s\|))^c$, and the discs are assumed to be open sets.

The SIR of the signal from the M-BS to the P-BS in DL backhaul is then given as,

$$\text{SIR}_{sm}(r_s, r_m) = \frac{P_m g_{r_s r_m} \|r_m - r_s\|^{-\alpha_m}}{I_s(r_s) + I_m(r_s) + \beta P_m}, \quad (3)$$

where the residual self-interference generated by the P-BS, being IBFD, is modeled as βP_m , β being a factor controlling the amount of self-interference. Though the self-interference channel

in some of the recent literature ([11], [24]) has been modeled as a Rician fading channel [25], this paper focuses on a simpler model. The idea is to get a handle on network coverage and rates given a self-interference suppressing IBFD radio, than to quantify the self-interference suppression capability of an IBFD radio.

2) *Macro cell association:* Assume that the typical user at the origin is associated to an M-BS denoted by point at $r'_m \in \Phi_m$. Let SIR_{um} denote the SIR of the signal from the M-BS to the user in DL access and is given by

$$\text{SIR}_{um}(r'_m) = \frac{P_m g_{or'_m} \|r'_m\|^{-\alpha_m}}{\hat{I}_s(o) + \hat{I}_m(o)}. \quad (4)$$

where $\hat{I}_s(o) = \sum_{z \in \Phi_s \cap B(o, \Delta_m r_m'^{\alpha_m/\alpha_s})} P_s g_{oz} \|z\|^{-\alpha_s}$ and $\hat{I}_m(o) = \sum_{z \in \Phi_m \cap B(o, r'_m)^c} P_m g_{oz} \|z\|^{-\alpha_m}$.

The next section analyzes coverage probability of a typical user in the given network.

III. COVERAGE

Coverage probability is defined as the probability that a randomly chosen user in the given network achieves an SIR greater than a given threshold. Let T_s , T_b and T_m be the SIR coverage thresholds for user to P-BS, P-BS to M-BS and user to M-BS links respectively. In the proposed setup, the effective coverage for a P-BS associated user would depend jointly on user to P-BS and P-BS to M-BS coverage probabilities denoted as $P_{u,s}(T_s)$, $P_{s,m}(T_b)$. For an M-BS associated user, coverage would only depend on the user to M-BS coverage probability denoted as $P_{u,m}(T_m)$. Using (1), the effective coverage probability for a user, $P_u^x(T_s, T_b, T_m)$, can now be defined as

$$P_u^x(T_s, T_b, T_m) = \Pr(\varepsilon_s) \cdot \Pr(\text{SIR}_{us} > T_s, \text{SIR}_{sm} > T_b \mid \varepsilon_s) + \Pr(\varepsilon_m) \cdot \Pr(\text{SIR}_{um} > T_m \mid \varepsilon_m), \quad (5)$$

where ε_m and ε_s denote events of M-BS and P-BS association and $x \in \{f, h\}$ denoting IBFD (full-duplex) or conventional FDD (half-duplex) operation. The joint distribution of r_m and r_s , that will be used in the evaluation of coverage probability is discussed next.

A. Joint probability density function of distance pair (r_s, r_m)

As mentioned above, the coverage under P-BS association implies a joint coverage probability over user to P-BS and P-BS to its backhauling M-BS links. This entails deriving a joint probability density function (pdf) of the distance pair (r_s, r_m) with respect to a typical user at the origin. When the user associates with a P-BS, the joint pdf $f(r_s, r_m)$ is derived for a

general Δ_m , that is, $\Delta_m \geq 1$ (typical, P-BS biased association) and $0 < \Delta_m < 1$ (negative P-BS bias). In Fig. 2a and Fig. 2b, the possible spatial configurations of the user, P-BS and M-BS are shown that occur because of various possible relative locations of the user associated P-BS and P-BS associated M-BS, with respect to the typical user at the origin. Instead of deriving the joint

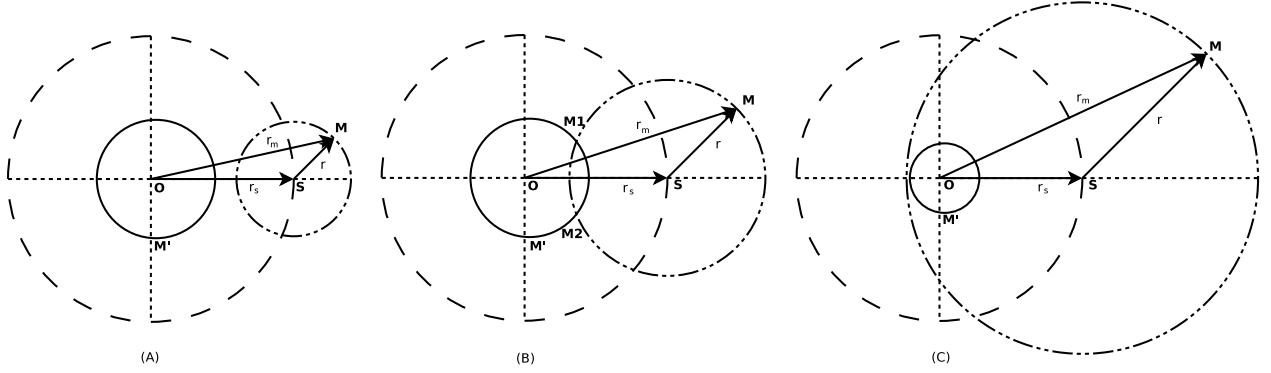


Fig. 2a: Network geometry for event ε_s With $\Delta_m \geq 1$, i.e., user biased towards P-BS tier. The three possible scenarios are as a result of different spatial locations of the P-BS and M-BS with respect to the typical user at the origin. When the user associates with a P-BS, coverage depends jointly on user to P-BS (for access) link and P-BS to M-BS (for backhaul) link. Given a P-BS S , found at distance r_s from O , the nearest M-BS to the user could be at a distance $\Delta_m^{-1} r_s^{\alpha_s / \alpha_m}$ from the origin O , denoted by OM' . The backhauling M-BS M could be found anywhere at a distance r_m from O , resulting in three different network geometries ((A), (B) and (C)) that define the joint density function of the P-BS and M-BS with respect to the typical user.

distribution for (r_s, r_m) , an equivalent distribution of (r_s, r) is derived. This is because of the occurrence of the term $\|r_m - r_s\|^{-\alpha}$ in the $\text{SIR}_{sm}(r_s, r_m)$ expression of equation 3. Replacing it with an equivalent $\|r\|^{-\alpha}$ simplifies the derivation of coverage expressions and so the joint distribution on (r_s, r) is used.

Lemma 1. *The joint density function of the access-backhaul distance pair, (r_s, r) , with respect to the typical user, given the bias factor $\Delta_m \geq 1$ is*

$$f(r_s, r) = \begin{cases} \frac{4e^{-\pi\left(r^2\lambda_m + \frac{r_s^2}{\Delta_m^2}\lambda_m + r_s^2\lambda_s\right)} \pi^2 r \lambda_m \left(\frac{r_s^{\alpha_m}}{\Delta_m^2} \alpha_s \lambda_m + r_s^2 \alpha_m \lambda_s\right)}{r_s \alpha_m}, & 0 < \|r\| \leq \nu_-(r_s, \Delta_m, \alpha_s, \alpha_m) \\ \frac{\partial \left(e^{-\lambda_s \pi r_s^2} e^{-\lambda_m \left(\pi(\Delta_m^{-1} r_s^{\alpha_s/\alpha_m})^2 + \pi r^2 - \text{lens}(M_1, M_2)\right)} \right)}{\partial r_s \partial r}, & \|r\| \in \nu_-^+(r_s, \Delta_m, \alpha_s, \alpha_m) \\ 4\pi^2 \lambda_m \lambda_s r r_s e^{-\pi(\lambda_m r^2 + \lambda_s r_s^2)}, & \|r\| \geq \nu_+(r_s, \Delta_m, \alpha_s, \alpha_m), \end{cases} \quad (6)$$

where

- $\nu_-(r_s, \Delta_m, \alpha_s, \alpha_m) \triangleq \|r_s\| - \Delta_m^{-1} \|r_s\|^{\alpha_s/\alpha_m}$
- $\nu_+(r_s, \Delta_m, \alpha_s, \alpha_m) \triangleq \|r_s\| + \Delta_m^{-1} \|r_s\|^{\alpha_s/\alpha_m}$
- $\nu_-^+(r_s, \Delta_m, \alpha_s, \alpha_m) \triangleq]\|r_s\| - \Delta_m^{-1} \|r_s\|^{\alpha_s/\alpha_m}, \|r_s\| + \Delta_m^{-1} \|r_s\|^{\alpha_s/\alpha_m}[$
- $\text{lens}(M_1, M_2)$ denotes the area of the lens formed between the points M_1 and M_2 in Case (B) of Fig. 2a

Proof: See Appendix A ■

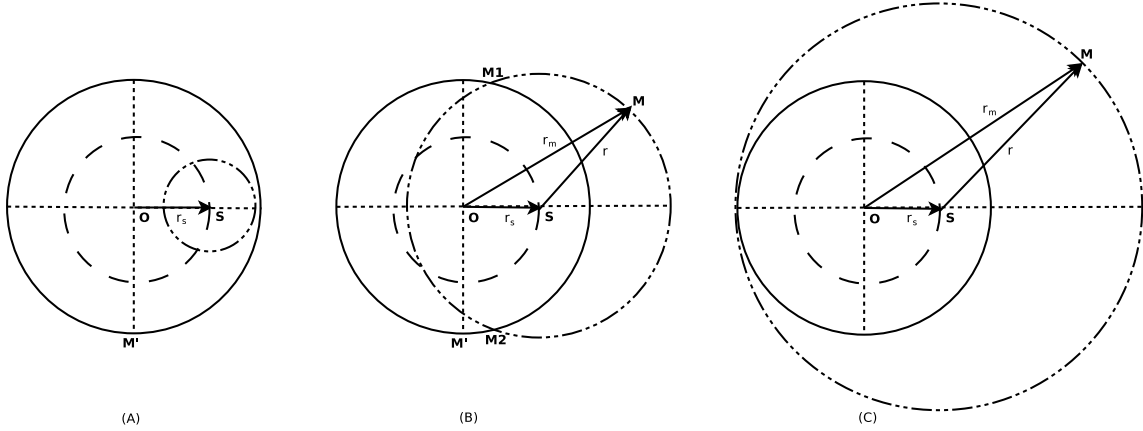


Fig. 2b: Network Geometry for Event ε_s With $0 < \Delta_m < 1$. The figure is similar to Fig. 2a, except that the user is biased towards the M-BS tier. Given the user associated P-BS is at a distance r_s from O , the nearest M-BS could only be at a distance $\geq \Delta_m^{-1} r_s^{\alpha_s/\alpha_m}$.

Lemma 2. *The joint density function of the access-backhaul distance pair, (r_s, r) , with respect to the typical user, given the bias factor $\Delta_m < 1$ is*

$$f(r_s, r) = \begin{cases} 0, & 0 < \|r\| \leq \mu_-(r_s, \Delta_m, \alpha_s, \alpha_m) \\ \frac{\partial \left(e^{-\lambda_s \pi r_s^2} e^{-\lambda_m \left(\pi (\Delta_m^{-1} r_s^{\alpha_s / \alpha_m})^2 + \pi r^2 - \text{lens}(M_1, M_2) \right)} \right)}{\partial r_s \partial r}, & \|r\| \in \mu_-^+(r_s, \Delta_m, \alpha_s, \alpha_m) \\ 4\pi^2 \lambda_m \lambda_s r r_s e^{-\pi(\lambda_m r^2 + \lambda_s r_s^2)}, & \|r\| \geq \mu_+(r_s, \Delta_m, \alpha_s, \alpha_m), \end{cases} \quad (7)$$

where

- $\mu_-(r_s, \Delta_m, \alpha_s, \alpha_m) \triangleq -\|r_s\| + \Delta_m^{-1} \|r_s\|^{\alpha_s / \alpha_m}$
- $\mu_+(r_s, \Delta_m, \alpha_s, \alpha_m) \triangleq \|r_s\| + \Delta_m^{-1} \|r_s\|^{\alpha_s / \alpha_m}$
- $\mu_-^+(r_s, \Delta_m, \alpha_s, \alpha_m) \triangleq]-\|r_s\| + \Delta_m^{-1} \|r_s\|^{\alpha_s / \alpha_m}, \|r_s\| + \Delta_m^{-1} \|r_s\|^{\alpha_s / \alpha_m}[$
- $\text{lens}(M_1, M_2)$ denotes the area of the lens formed between the points M_1 and M_2 in Case (B) of Fig. 2b

Proof: See Appendix A ■

B. Small Cell Coverage in IBFD

In this section, the coverage probability of a typical user under P-BS is derived. Coverage under P-BS is denoted as $P_{u,s}^f(T_s, T_b)$ and the corresponding geometry of the node locations is depicted in Fig. 3.

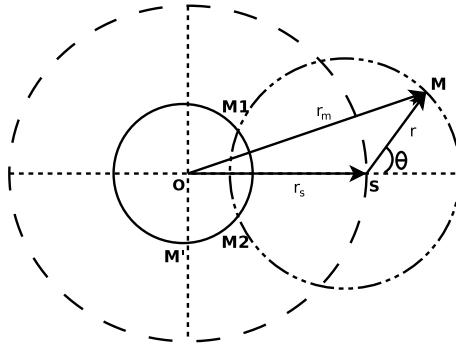


Fig. 3: An instance of user associating with P-BS

A typical user located at the origin o associates with a P-BS (S in Fig. 3) at a distance r_s . From (1), it follows that there is no M-BS inside a ball of radius $OM' = \Delta_m^{-1} r_s^{\alpha_s / \alpha_m}$ centered

at the origin o . For the backhaul, the P-BS S connects to the nearest M-BS (M in Fig. 3) at a distance r_m from o . The backhaul distance from the P-BS S to the backhauling M-BS M is r . In IBFD mode, the user when associated with the P-BS, will receive interference from other P-BSs as well as all the M-BSs. Let $g(s, x, \alpha)$ be defined as

$$g(s, x, \alpha) = \frac{1}{1 + s\|x\|^{-\alpha}}.$$

Lemma 3. *The probability of coverage for a user associated with a P-BS in the given two-tier IBFD network is*

$$P_{u,s}^f(T_s, T_b) = \int_0^{2\pi} \int_{r_s > 0, r > 0} e^{-\lambda_s \int_{\Phi_s \cap A_1^c} 1 - g(s_1, z, \alpha_s) g(s_2, z - r_s, \alpha_s) dz - \lambda_m \int_{\Phi_m \cap A_2^c} 1 - g(s'_1, v, \alpha_m) g(s'_2, v - r_s, \alpha_m) dv - \beta s_2} g(s'_1, r_m, \alpha_m) f(r_s, r) dr_s dr d\theta \quad (8)$$

where, $A_1 = B(o, r_s)$, $s_1 = T_s \|r_s\|^{\alpha_s}$, $s_2 = \frac{T_b}{P_m} \|r\|^{\alpha_m} P_s$, $r_m = \sqrt{r_s^2 + r^2 + 2r_s r \cos \theta}$, $A_2 = (B(o, \Delta_m^{-1} r_s^{\alpha_s / \alpha_m}) \cup B(r_s, \|r\|))$, $s'_1 = \frac{T_s}{P_s} \|r_s\|^{\alpha_s} P_m$, and $s'_2 = T_b \|r\|^{\alpha_m}$.

Proof: See Appendix B ■

The integral in Lemma 3 can be divided into three integrals over the variables θ, r_s and r corresponding to the cases (A), (B) or (C) of Fig. 2a and Fig. 2b. Of particular interest, is the density function of Case (B), where the backhaul and the inner macro discs intersect. Backhaul disc is the one that has distance from the serving P-BS to the serving P-BS's backhauling M-BS as the radius. Though the expression for it has been derived as in (6), it is hard to compute numerically. Therefore, probability for the intersection case is analyzed below.

Let \mathcal{C} and \mathcal{I} denote events *user covered under P-BS* and *intersection of the backhaul and the inner macro discs* of Fig. 2a respectively. Then \mathcal{I} is defined as

$$\mathcal{I} \triangleq \|r - \Delta_m^{-1} r_s^{\alpha_s / \alpha_m}\| \leq \|r_s\| \leq \|r + \Delta_m^{-1} r_s^{\alpha_s / \alpha_m}\|.$$

Using Bayes rule, the probability $\Pr(\mathcal{I} | \mathcal{C})$ is

$$\Pr(\mathcal{I} | \mathcal{C}) = \frac{\Pr(\mathcal{C}, \mathcal{I})}{\Pr(\mathcal{C})}. \quad (9)$$

The expressions for $\Pr(\mathcal{C}, \mathcal{I})$ and $\Pr(\mathcal{C})$ are already derived in equation (8).

The plot in Fig. 4 reveals useful information about the network topology. For the given system model, at reasonably high biasing towards the P-BS, the system mostly remains in the state of

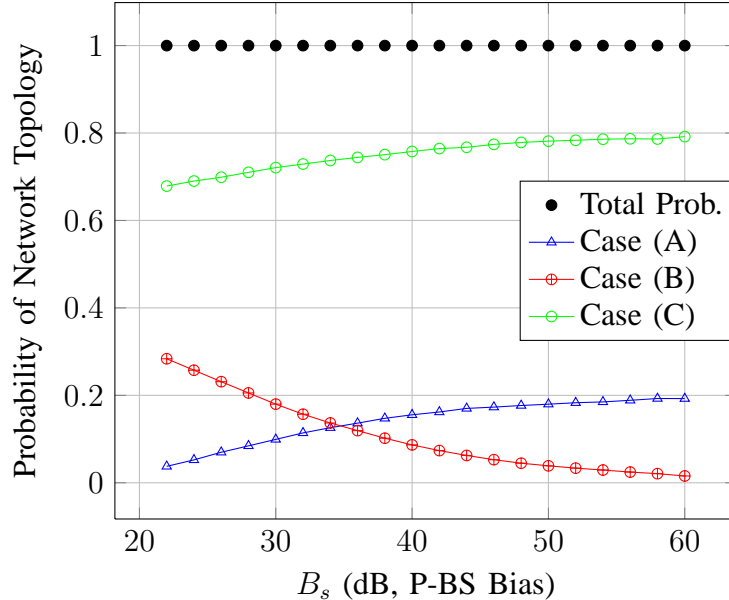


Fig. 4: Probability of Network Topology vs. P-BS Bias in Small cell association ($T_m = T_s = T_b = -10$ dB, $B_m = 0$ dB, $P_m = 22$ dB, $P_s = 0$ dB, $\alpha_m = 2.8$, $\alpha_s = 4$, $\lambda_s = 4\lambda_m$). Each plot shows the probability of the network being in a particular geometry. Case (A) denotes *Zero Intersect. Prob.* curve that depicts the probability of the inner macro and the backhaul disc having zero intersection, Case (B) (*Intersect Prob.*) curve depicts the probability of the inner macro and the backhaul disc intersecting and Case (C) (*Engulf. Prob.*) curve depicts the probability of the backhaul disc engulfing the inner macro disc in event of small cell association of Fig. 2a. Notice that in the limit of bias towards P-BS, i.e. high bias towards small cell tier, the *Intersect Prob.* curve goes to 0, rendering numerical computations much easier.

Case (A) or Case (C) of Fig. 2a. Therefore, coverage could be approximated by averaging over system states of Case (A) and Case (C) alone, which is much more tractable than using the entire joint density function—a rather complex function to evaluate. The plot also makes practical sense, as a HetNet under typical circumstances, would be operated in a mode highly biased towards the P-BSs [26], [27].

C. Macro Cell Coverage in IBFD

Coverage probability for a user associated with an M-BS is derived here. For such a user, there is only a single active link (user-M-BS) since the M-BSs are fiber backhauled to the core network. In this case, it is more convenient to calculate coverage as $\Pr(\text{SIR}_{um} > T_m, \varepsilon_m)$ directly rather than the conditional coverage based on the event ε_m .

Lemma 4. *The probability of coverage for a user associated with a M-BS in the given two-tier*

IBFD network is denoted by $P_{u,m}^f(T_m)$ and is given as

$$P_{u,m}^f(T_m) = \int_{r'_m=0}^{\infty} \int_{r_s=\Delta_s r'_m{}^{\alpha_m/\alpha_s}}^{\infty} F(\Phi_m, \Phi_s) f(r'_m, r_s) dr'_m dr_s, \quad (10)$$

where $f(r'_m, r_s)$ denotes the density function of the nearest M-BS and P-BS and is given as:

$$f(r'_m, r_s) = 2\pi\lambda_m r'_m e^{-\pi\lambda_m r'_m{}^2} 2\pi\lambda_s r_s e^{-\pi\lambda_s r_s^2} \quad (11)$$

and

$$F(\Phi_m, \Phi_s) = e^{-\pi r'_m{}^2 \lambda_m T_m^{2/\alpha_m} \int_{T_m^{-2/\alpha_m}}^{\infty} \frac{1}{1+t^{\alpha_m/2}} dt} e^{-\pi r_m^{2\alpha_m/\alpha_s} \lambda_s \left(\frac{P_s T_m}{P_m}\right)^{\frac{2}{\alpha_s}} \int_{\left(\frac{B_s}{B_m T_m}\right)^{\frac{2}{\alpha_s}}}^{\infty} \frac{1}{1+t^{\alpha_s/2}} dt}.$$

Proof: See Appendix C ■

D. Small Cell Coverage in FDD

In FDD case the frequency resources are orthogonalized between the access and backhaul tiers and so interference to a user in the DL is much reduced. This comes at the cost of halving the spectrum for access and backhaul link each.

Lemma 5. *The probability of coverage for a user associated with a P-BS in the given two-tier FDD network is denoted by $P_{u,s}^h(T_s, T_b)$ and given as*

$$P_{u,s}^h(T_s, T_b) = \int_{\mathbb{R}^2} e^{-\lambda_s \int_{z \in \Phi_s \cap A_1^c} 1-g(\|r_s\|^{\alpha_s} T_s, z, \alpha_s) dz - \lambda_m \int_{v \in \Phi_m \cap A_2^c} 1-g(\|r\|^{\alpha_m} T_b, v-r_s, \alpha_m) dv} f(r_s, r) dr_s dr, \quad (12)$$

where $g(s, x, \alpha) = \frac{1}{1+s\|x\|^{-\alpha}}$, $A_1 = B(o, r_s)$, $A_2 = (B(o, \Delta_m^{-1} r_s^{\alpha_s/\alpha_m}) \cup B(r_s, \|r\|))$.

Proof:

$$\Pr(\text{SIR}_{us} > T_s, \text{SIR}_{sm} > T_b \mid \varepsilon_s) = \mathbb{E}_{r_s, r} \left[\underbrace{\Pr(\text{SIR}_{us} > T_s, \text{SIR}_{sm} > T_b \mid r_s, r)}_{P_{u,s}^h(T_s, T_b)} \right].$$

The representation of conditioning on points r_s and r is dropped in interest of better clarity, for the following derivation. For FDD case, the user (or P-BS) receives interference only from the tier that it is associated with.

$$P'_{u,s}(T_s, T_b) = \Pr \left(\frac{P_s g_{or_s} \|r_s\|^{-\alpha_s}}{\sum_{z \in A_1^c} P_s g_{oz} \|z\|^{-\alpha_s}} > T_s, \frac{P_m g_{r_s r_m} \|r\|^{-\alpha_m}}{\sum_{z \in A_2^c} P_m g_{r_s z} \|z - r_s\|^{-\alpha_m}} > T_b \right),$$

Proceeding in the same way as in Appendix B for IBFD coverage, the expression for coverage in the FDD network could be calculated to be as (12). ■

E. Macro Cell Coverage in FDD

Users associated with the macro cells in FDD case see interference only from the macro cells. The coverage expression uses r'_m and r_s for nearest P-BS and M-BS respectively as in IBFD macro cell coverage case. So macro cell coverage is calculated as $\Pr(\text{SIR}_{um} > T_m, \varepsilon_m)$ directly.

Lemma 6. *The probability of coverage for a user associated with a M-BS in the given two-tier FDD network is denoted by $P'_{u,m}(T_m)$ and given as,*

$$P'_{u,m}(T_m) = \int_{r'_m=0}^{\infty} \int_{r_s=\Delta_s r'_m}^{\infty} e^{-\pi r'_m{}^2 \lambda_m T_m^{2/\alpha_m}} \int_{T_m^{-2/\alpha_m}}^{\infty} \frac{1}{1+t^{\alpha_m/2}} dt f(r'_m, r_s) dr'_m dr_s, \quad (13)$$

where $f(r'_m, r_s)$ is defined as in (11).

Proof: Lemma 6 directly follows from the proof given for Lemma 4, considering a user associated with a given tier will receive interference only from that tier. ■

IV. AVERAGE RATE

This section focuses on the the achievable rate for a typical user located at the origin conditioned on the user being under coverage. For full-duplex case the entire $1 Hz$ is used for self-backhauling as well as access links by the P-BSs. At the M-BSs, ηHz is used for the backhauling link to P-BSs and an orthogonal $(1 - \eta) Hz$ for direct access link to the user. The arrangement is similar for half-duplex case, but for the fact that the spectrum is orthogonalized as $0.5 Hz$ each, for access and backhaul links with respect to the P-BSs. Notice that the rate in DL for users connected to the P-BS is the minimum of rates on the M-BS to P-BS and the P-BS to user links. This is taken into account by the derivation that follows. Let an event, that the user is

covered, be defined as $\{\text{Coverage}\} \triangleq \mathbf{1}(\varepsilon_m)\{\text{SIR}_{um} > T_m\} \cup \mathbf{1}(\varepsilon_s)\{\text{SIR}_{us} > T_s, \text{SIR}_{sm} > T_b\}$, where $\mathbf{1}(\varepsilon)$ denotes an indicator random variable for event ε ,

$$\begin{aligned} \mathbb{E}[R_u | \text{Coverage}] &= \frac{1}{\Pr\{\text{Coverage}\}} (\mathbb{E}[R_{um} | \text{SIR}_{um} > T_m] \Pr(\text{SIR}_{um} > T_m) + \\ &\quad \mathbb{E}[\min(R_{us}, R_{sm}) | \text{SIR}_{us} > T_s, \text{SIR}_{sm} > T_b] \Pr(\text{SIR}_{us} > T_s, \text{SIR}_{sm} > T_b).) \end{aligned} \quad (14)$$

A. M-BS to User Rate (R_{um})

The expectation in the first term in (14) is calculated as follows. Let $\bar{\eta} = (1 - \eta)$. Let $\bar{\eta} Hz$ be used at the M-BSs for access to user. Then,

$$\mathbb{E}[R_{um} | \text{SIR}_{um} > T_m] = \frac{\bar{\eta}}{\Pr(\text{SIR}_{um} > T_m)} \int_{t>0} \Pr(\text{SIR}_{um} > \max(2^t - 1, T_m)) dt, \quad (15)$$

Proof: See Appendix D ■

The coverage expression for M-BS-user case, given by (10), can be used in (15) to obtain the average conditional rates.

B. M-BS to P-BS to User Rate ($\min(R_{us}, R_{sm})$)

The expectation in the second term in (14) is computed now. For notational simplicity, let $\{\text{SIR}_{us,sm} > T_{s,b}\} \triangleq \{\text{SIR}_{us} > T_s, \text{SIR}_{sm} > T_b\}$. On an average, each macro cell is assumed to backhaul n small cells, where $n = \lambda_s/\lambda_m$. This means that on the backhaul link, the rate to each P-BS will get reduced by a factor of n , besides being multiplied by η , which is the amount of bandwidth from $1 Hz$, that is allocated by the M-BSs for backhauling P-BSs.

$$\begin{aligned} \mathbb{E}[\min(R_{us}, R_{sm}) | \text{SIR}_{us,sm} > T_{s,b}] &= \\ &= \frac{1}{\Pr(\text{SIR}_{us,sm} > T_{s,b})} \int_{t>0} \Pr\left(\text{SIR}_{us} > \max(2^t - 1, T_s), \text{SIR}_{sm} > \max(2^{\frac{nt}{\eta}} - 1, T_b)\right) dt. \end{aligned} \quad (16)$$

Proof: See Appendix E ■

The average conditional rate could be similarly calculated for the FDD system keeping note of the fact that the bandwidth gets split into $0.5 Hz$ each for the backhaul and the access links, which essentially, at least theoretically, must halve the rates for a FDD system in comparison to a IBFD system.

V. NUMERICAL RESULTS

This section numerically computes the coverage expressions provided in the previous sections and compares them with Monte Carlo simulations. The parameters used for Monte-Carlo simulation are the same as mentioned in section II-C. Simulation is done with PPPs Φ_s and Φ_m on an area of 60×60 square units with 14400 and 3600 nodes, respectively. All simulations are shown with the self-interference factor $\beta = 0$ dB, path loss exponent for the M-BS tier, $\alpha_m = 2.8$ and for the P-BS tier, $\alpha_s = 4$, unless mentioned otherwise. Transmit powers of M-BS and P-BS are proportionally considered as $P_m = 150$ and $P_s = 1$ in accordance with powers of 46 dBm and 24 dBm respectively for wide-area and local-area BS [28]. Bias towards M-BS $B_m = 0$ dB, unless mentioned otherwise.

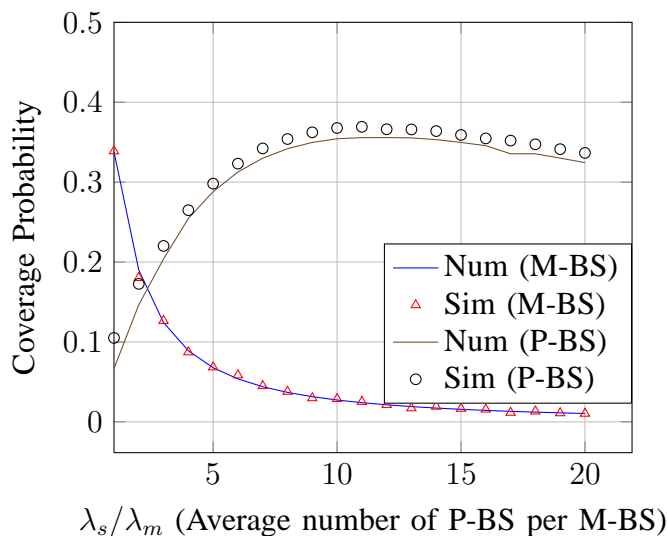


Fig. 5: Coverage Probability vs. Small Cell Density. ($T_m = T_s = T_b = -10$ dB. $B_s = 22$ dB $\lambda_m = 1$, $\alpha_m = 2.8$, $\alpha_s = 4$)

The coverage probability is plotted with respect to different parameters in Fig. 5 and Fig. 6. A close match between the simulations and the numerical evaluation of the theoretical expressions is seen. This establishes the validity of the derived analytical framework, that is tractable and quick in computing the network coverage trends in the proposed IBFD self-backhauling network.

The SIR for a typical user in a IBFD self-backhauling network is far lesser than that of its FDD counterpart, which results in much less coverage for a IBFD network. This is primarily because of the inter-tier interference in addition to the intra-tier interferers (intra-tier interference

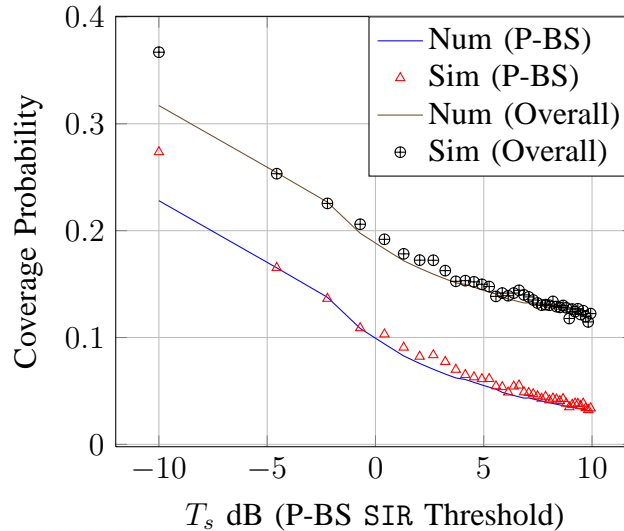


Fig. 6: Coverage Probability vs. P-BS SIR Threshold. ($T_m = T_b = -10$ dB. $B_s = 22$ dB, $\alpha_m = 2.8$, $\alpha_s = 4$)

present in FDD network too) in an IBFD network. More biasing towards the P-BS tier requires more backhauling on the same spectrum, eventually resulting in increased interference to the access links.

Plots of Fig. 7 and Fig. 8 show the coverage variation versus the P-BS SIR threshold and ratio of densities of P-BS and M-BS. As expected, the coverage for both IBFD and FDD cases decreases with increasing T_s . As T_s is increased, users associated with the P-BS do not get sufficient SIR for coverage. This implies the coverage mostly corresponds to that provided by the M-BS and hence at large values of T_s the two curves in Fig. 7 approach each other.

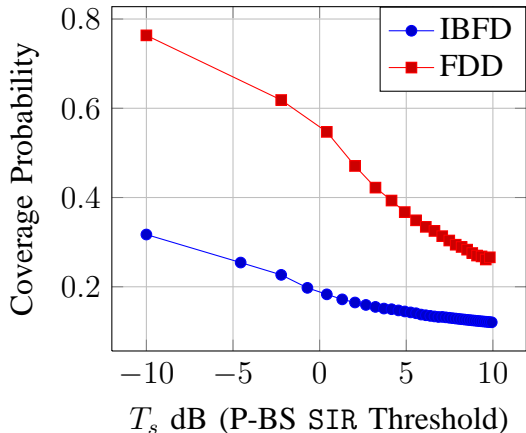


Fig. 7: $T_m = T_b = -10$ dB, $\lambda_s = 4\lambda_m$, $B_s = 22$ dB. As expected, coverage decreases with increasing SIR thresholds. The two curves converge asymptotically as increasing T_s beyond a certain range results in a virtually macro-only network.

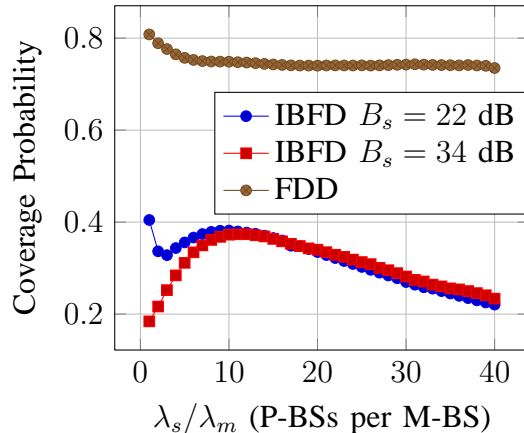


Fig. 8: $T_m = T_b = T_s = -10$ dB. With higher B_s , there is an optimal P-BS density achieving maximum coverage. At higher biasing, the P-BS density should be commensurate with the B_s values so as to fully utilize the biasing effect.

In Fig. 8, the FDD coverage curve is in accordance with the findings in [29], in that the coverage remains almost constant with increasing density of P-BSs. For the IBFD curve, the findings are different. For high biasing towards P-BS, there is an optimal density that maximizes the coverage, whereas for reasonably lower B_s coverage decreases with increasing P-BS density. The reason is not very apparent by the total coverage plot of Fig. 8, but only by inspecting the coverage within backhaul and access layers. It is the coverage under P-BSs that gives the shape of the high B_s plot in Fig. 8. Coverage under P-BS is composed of two probabilities—user coverage under P-BS and the P-BS coverage under a backhauling M-BS as shown in Fig. 9. The plot in Fig. 9 shows the individual coverage probabilities of M-BS to P-BS (backhaul) and P-BS to user (access) links with varying P-BS density to gain insight into the behavior of the coverage plot in Fig. 8. These plots bring out fundamental scaling trends in such a self-backhauling network. They show that the net coverage under P-BS increases with P-BS density till an optimum is reached. This is because during this increase in density, effective bias towards the P-BS increases and more users associate and subsequently get covered under P-BSs, albeit with lower SIR.

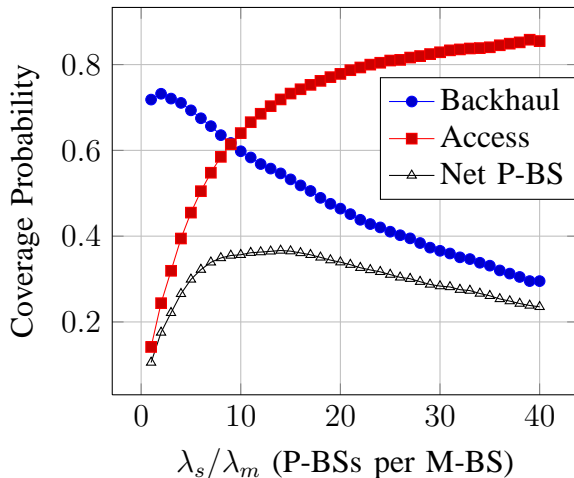


Fig. 9: $T_m = T_b = T_s = -10$ dB, $B_s = 34$ dB. Net P-BS coverage curve is shaped by two probabilities, P-BS to user and M-BS to P-BS coverage.

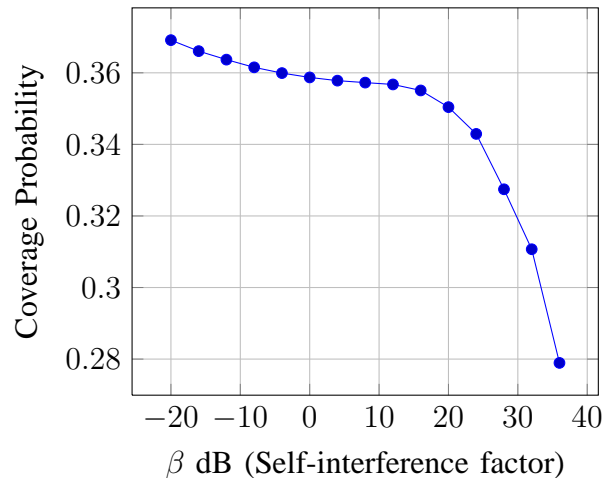


Fig. 10: $T_m = T_b = T_s = -10$ dB, $B_s = 22$ dB, $\lambda_s = 4\lambda_m$. Coverage with varying β . As expected, coverage reduces with reducing self-interference cancellation capability.

Moreover, there is scope for the M-BSs to cater to more P-BSs for backhauling. The result is an increase in coverage. Beyond the optimum coverage point, user coverage under P-BSs starts to stagnate but the backhauling coverage drops steeply. Stagnation in P-BS to user coverage is due to the fact that at high P-BS density, users mostly associate with P-BS. Then, the network behaves as if a single tier network with increasing BS density which is known to be constant [29]. On the other hand the backhaul coverage drops due to the increasing interference that the access links of the P-BS pose to the backhaul links of the P-BS. This effectively results in an overall decrease in the coverage under P-BSs. The same is not true of the FDD counterpart of such a network. In FDD case, backhauling links do not interfere with the access links. With increasing P-BS density, an increasing P-BS coverage balances a declining M-BS coverage to give an almost constant net coverage.

As expected, Fig. 10 shows the degradation of coverage with increasing self-interference factor at the P-BS.

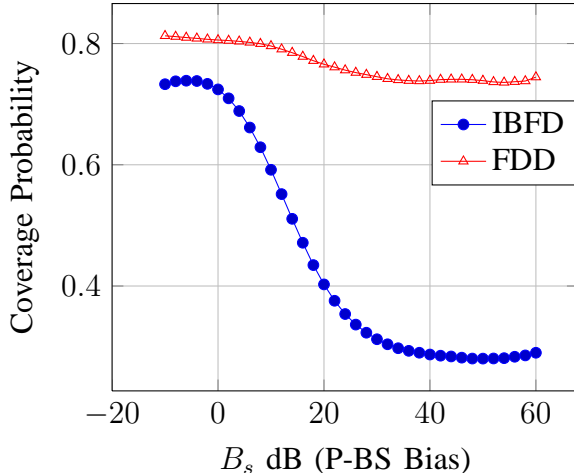


Fig. 11: $T_m = T_b = T_s = -10$ dB, $\lambda_s = 4\lambda_m$. The coverage falls when users are biased to associate to P-BS, even with lesser SIR than they see with the M-BS. This stagnates at a point where almost all users are associated to P-BS.

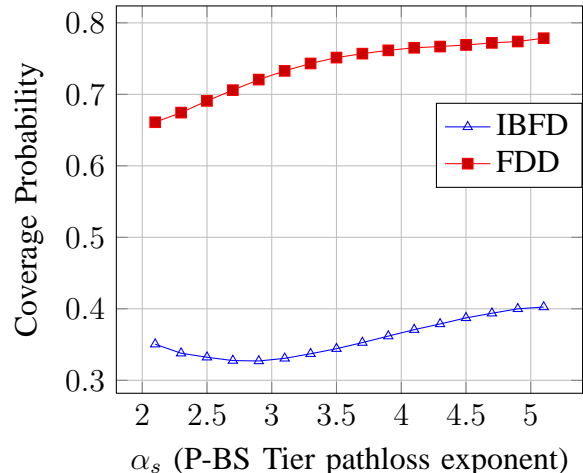


Fig. 12: $T_m = T_b = T_s = -10$ dB, $\lambda_s = 4\lambda_m$. The coverage increases with increasing pathloss exponent α_s . A larger pathloss exponent is helpful in a heterogeneous network with reasonably high density, as it mitigates interference in a dense network.

The plot in Fig. 11 shows that biasing more towards the P-BS forces the users to associate with them even when the SIR received from them is lesser than that from the M-BS. This results in decrease in coverage until a point where mostly all users are associated with the P-BS tier only and therefore the coverage stagnates. The plot also suggests that the decrease in coverage in the IBFD case is much steeper than in the FDD case. This is because in the IBFD case, the P-BS tier receives maximum interference—from other M-BSs as well as all the P-BSs. For a user to be biased in associating with a P-BS in a IBFD case is essentially forcing it to accept a much weaker SIR link than in the case of FDD operation. Hence the coverage for a user in IBFD operation degrades much more rapidly than in the FDD case. The plot of Fig. 12 shows that higher pathloss exponent helps a dense P-BS deployment as it creates virtual cell splitting. The plot shows an initial dip in coverage, but only till $\alpha_s = \alpha_m = 2.8$.

The following plots show the variation of average conditional rate of a typical user in a IBFD and FDD self-backhauling network. All rates are calculated keeping the bandwidth partitioning parameter $\eta = 0.8$. Since the available bandwidth is entirely used by the P-BSs and M-BSs in IBFD network, the rate in IBFD networks, typically tends to twice that of FDD networks. As the interference in IBFD network is more than the conventional FDD network, the rate is not

twice that of the FDD networks.

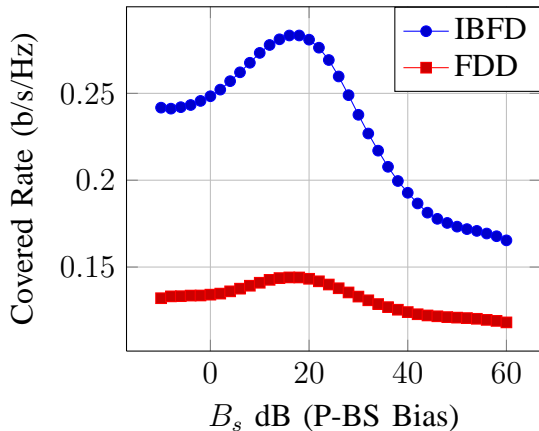


Fig. 13: $T_m = T_b = T_s = -10$ dB, $\lambda_s = 4\lambda_m$. Covered rate increases higher B_s until an optimal point, after which it reduces as the P-BS density remains constant.

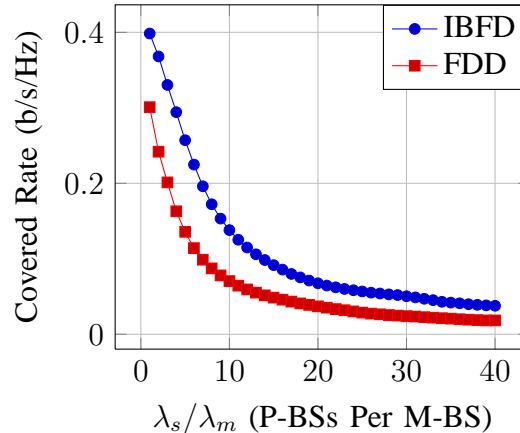


Fig. 14: $T_m = T_b = T_s = -10$ dB, $B_s = 22$ dB. Denser P-BSs limit the backhaul bandwidth available per P-BS and the covered rate falls.

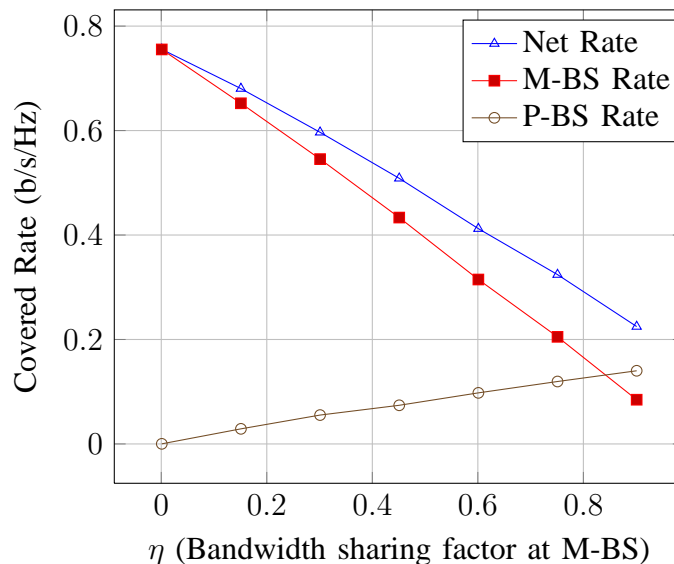


Fig. 15: Covered Rate vs. Bandwidth Sharing at M-BS. ($T_m = T_s = T_b = -10$ dB, $B_s = 22$ dB), Available bandwidth at the M-BS needs to be segregated into resources used for backhauling P-BS and for direct access to users.

The plots in Fig. 13 and Fig. 14 show the variation of rate with varying T_s and λ_s . As expected, the average normalized rate increases with increasing T_s and decreases with increasing P-BS

density. In Fig. 14, increasing P-BS density reduces the backhaul bandwidth per P-BS and the rate (which is the minimum over backhaul and access link) also reduces. Thus, the interference from the backhaul to the access links as well as the division of bandwidth at the backhauling M-BS, are two major limitations in the considered IBFD self-backhauling network.

The plot in Fig. 13 shows that with $\eta = 0.8$, there exists a bias point that achieves the maximum average rate. Since the density of P-BSs is four times that of M-BSs, there exists a point where all the P-BSs are fully utilized to deliver rate to the typical user and hence the shape of the curve. Beyond this point, as the users are forced to associate to a weaker SIR link from the P-BS, the average rate begins to fall. The results obtained in this section indicate two major impediments to achieving the full potential of IBFD self-backhauling networks that are *inter-tier interference* from the backhaul to access links and *bandwidth division* at the M-BS to accommodate backhauling resources for multiple P-BSs.

VI. CONCLUSION

This work proposed and analyzed a self-backhauling HetNet architecture for IBFD as well as traditional FDD enabled base-stations. A tractable and quick-to-compute analytical model for network wide coverage is derived and shown to match simulation results. The paper shows that the proposed IBFD self-backhauling network suffers from limitations posed by the inter-tier interference and the bandwidth division at the backhauling M-BS. Though IBFD capability helps improve the average rates (conditioned on user being covered) by a factor less than double, the coverage in such a network is close to half of its FDD counterpart. Analytical framework for exact quantification of coverage under varying parameters such as P-BS density, bias, pathloss exponent, etc. has been derived. The proposed architecture requires only small cells to be IBFD-enabled, which is practically more suitable than IBFD operation on M-BS and user devices owing to their high transmit powers and small form factors, respectively. The paper uses an example IBFD network for clear exposition though similar analysis holds for time-division duplexed (TDD) networks, for instance, by replacing frequencies f_1 and f_2 by time-slots t_1 and t_2 .

REFERENCES

- [1] METIS, "Mobile and wireless communications Enablers for the Twenty-twenty Information Society," tech. rep., EU 7th Framework Programme Project, Mar. 2013.

- [2] A. Damnjanovic, J. Montojo, Y. Wei, T. Ji, T. Luo, M. Vajapeyam, T. Yoo, O. Song, and D. Malladi, "A survey on 3gpp heterogeneous networks," *Wireless Communications, IEEE*, vol. 18, pp. 10–21, June 2011.
- [3] ETSI, "LTE;Scenarios and requirements for small cell enhancements for E-UTRA and E-UTRAN, 3GPP TR 36.932 version 12.1.0 Release 12," TR 36.932, European Telecommunications Standards Institute (ETSI), Oct. 2014.
- [4] R. Schwartz and M. Rice, "Rethinking Small Cell Backhaul," tech. rep., Wireless2020, July 2012.
- [5] A. Nadh, J. Samuel, A. Sharma, S. Aniruddhan, and R. K. Ganti, "A linearization technique for self-interference cancellation in full-duplex radios," *arXiv preprint arXiv:1605.01345*, 2016.
- [6] A. Nadh, A. Sharma, S. Aniruddhan, and R. K. Ganti, "A taylor series approximation technique for self-interference cancellation in full-duplex radios," in *2016 Twenty Second National Conference on Communication (NCC)*, pp. 1–6, March 2016.
- [7] M. Jain, J. I. Choi, T. Kim, D. Bharadia, S. Seth, K. Srinivasan, P. Levis, S. Katti, and P. Sinha, "Practical, real-time, full duplex wireless," in *Proceedings of the 17th Annual International Conference on Mobile Computing and Networking, MobiCom '11*, (New York, NY, USA), pp. 301–312, ACM, 2011.
- [8] M. Duarte and A. Sabharwal, "Full-duplex wireless communications using off-the-shelf radios: Feasibility and first results," in *Signals, Systems and Computers (ASILOMAR), 2010 Conference Record of the Forty Fourth Asilomar Conference on*, pp. 1558–1562, Nov 2010.
- [9] S. Hong, J. Brand, J. Choi, M. Jain, J. Mehlman, S. Katti, and P. Levis, "Applications of self-interference cancellation in 5g and beyond," *Communications Magazine, IEEE*, vol. 52, pp. 114–121, February 2014.
- [10] B. Li and P. Liang, "Small cell in-band wireless backhaul in massive MIMO systems: A cooperation of next-generation techniques," *CoRR*, vol. abs/1402.2603, 2014.
- [11] I. Atzeni and M. Kountouris, "Full-duplex mimo small-cell networks: Performance analysis," *arXiv preprint arXiv:1509.05506*, 2015.
- [12] S. Goyal, P. Liu, S. Hua, and S. Panwar, "Analyzing a full-duplex cellular system," in *Information Sciences and Systems (CISS), 2013 47th Annual Conference on*, pp. 1–6, March 2013.
- [13] H. Kim, S. Lim, H. Wang, and D. Hong, "Optimal power allocation and outage analysis for cognitive full duplex relay systems," *Wireless Communications, IEEE Transactions on*, vol. 11, pp. 3754–3765, October 2012.
- [14] S. Barghi, A. Khojastepour, K. Sundaresan, and S. Rangarajan, "Characterizing the throughput gain of single cell mimo wireless systems with full duplex radios," in *Modeling and Optimization in Mobile, Ad Hoc and Wireless Networks (WiOpt), 2012 10th International Symposium on*, pp. 68–74, May 2012.
- [15] H. Ju, S. Lim, D. Kim, H. Poor, and D. Hong, "Full duplexity in beamforming-based multi-hop relay networks," *Selected Areas in Communications, IEEE Journal on*, vol. 30, pp. 1554–1565, September 2012.
- [16] V. Aggarwal, M. Duarte, A. Sabharwal, and N. Shankaranarayanan, "Full- or half-duplex? a capacity analysis with bounded radio resources," in *Information Theory Workshop (ITW), 2012 IEEE*, pp. 207–211, Sept 2012.
- [17] T. Riihonen, S. Werner, and R. Wichman, "Hybrid full-duplex/half-duplex relaying with transmit power adaptation," *Wireless Communications, IEEE Transactions on*, vol. 10, pp. 3074–3085, September 2011.
- [18] S. Singh, M. Kulkarni, A. Ghosh, and J. Andrews, "Tractable model for rate in self-backhauled millimeter wave cellular networks," 2014.
- [19] A. Sharma, R. K. Ganti, and J. K. Milleth, "Performance analysis of full duplex self-backhauling cellular network," in *2016 IEEE International Conference on Communications (ICC)*, pp. 1–6, May 2016.
- [20] D. Stoyan, W. Kendall, J. Mecke, and D. Kendall, *Stochastic Geometry and Its Applications*. John Wiley and Sons, 1996.
- [21] R. K. Ganti, "Stochastic geometry and wireless networks," 2012.

- [22] H. Dhillon, R. , F. Baccelli, and J. Andrews, “Modeling and analysis of k-tier downlink heterogeneous cellular networks,” *Selected Areas in Communications, IEEE Journal on*, vol. 30, pp. 550–560, April 2012.
- [23] H.-S. Jo, Y. J. Sang, P. Xia, and J. Andrews, “Heterogeneous cellular networks with flexible cell association: A comprehensive downlink sinr analysis,” *Wireless Communications, IEEE Transactions on*, vol. 11, pp. 3484–3495, October 2012.
- [24] M. Duarte, C. Dick, and A. Sabharwal, “Experiment-driven characterization of full-duplex wireless systems,” *Wireless Communications, IEEE Transactions on*, vol. 11, pp. 4296–4307, December 2012.
- [25] M. K. Simon and M.-S. Alouini, *Digital communication over fading channels*, vol. 95. John Wiley & Sons, 2005.
- [26] A. Damnjanovic, J. Montojo, Y. Wei, T. Ji, T. Luo, M. Vajapeyam, T. Yoo, O. Song, and D. Malladi, “A survey on 3gpp heterogeneous networks,” *Wireless Communications, IEEE*, vol. 18, no. 3, pp. 10–21, 2011.
- [27] P. T. Airpsan, “Small Cell LTE Deployments Tightly Integrating Access and Backhaul,” tech. rep., Small Cells Americas, November 2012.
- [28] 3GPP, “3rd Generation Partnership Project; Technical Specification Group Radio Access Network; Evolved Universal Terrestrial Radio Access (E-UTRA); Base Station (BS) radio transmission and reception (Release 13),” TS 36.104, 3rd Generation Partnership Project (3GPP), July 2015.
- [29] J. Andrews, F. Baccelli, and R. Ganti, “A tractable approach to coverage and rate in cellular networks,” *Communications, IEEE Transactions on*, vol. 59, pp. 3122–3134, November 2011.
- [30] E. W. Weisstein, “Circle-circle intersection, from mathworld—a wolfram web resource,”

APPENDIX A

JOINT PDF OF DISTANCE PAIR (r_s, r)

The joint pdf of the distance pair (r_s, r) that characterizes the joint density of the access-backhaul nodes is derived here.

1) $\Delta_m \geq 1$: Considered first is the arrangement as shown in Fig. 2a. The representations in Fig. 2a depict cases depending on the location of the backhauling M-BS, provided the user associates with the P-BS at a point r_s . Parts (A), (B) and (C) represent cases where the backhaul disc (circle with radius $\|r\|$) and the inner macro disc (circle with radius denoted by $OM' = \Delta_m^{-1} r_s^{\alpha_s/\alpha_m}$)

- do not intersect
- have finite intersection area
- represent a single disc (i.e. the backhaul disc engulfs the inner macro disc)

Following this, the pdf is composed of three sub-parts depending on where the backhauling M-BS is found.

- *Case (A)*: $0 < \|r\| \leq \nu_-(r_s, \Delta_m, \alpha_s, \alpha_m)$ In this case the density function is given by the void probabilities [20] of Φ_s over $\Phi_s \cap B(o, \|r_s\|)^c$ and of Φ_m over $\Phi_m \cap (B(o, \|\Delta_m^{-1} r_s^{\alpha_s/\alpha_m}\|) \cup$

$B(r_s, \|r\|)^c$ i.e.

$$\begin{aligned}
f(r_s, r) &= \frac{\partial F(r_s, r)}{\partial r_s \partial r} \\
&= \frac{\partial \left(e^{-\lambda_s \pi r_s^2} e^{-\lambda_m \pi \left((\Delta_m^{-1} r_s^{\alpha_s / \alpha_m})^2 + r^2 \right)} \right)}{\partial r_s \partial r} \\
&= \frac{4e^{-\pi \left(r^2 \lambda_m + \frac{r_s^{\frac{2\alpha_s}{\alpha_m}}}{\Delta_m} \lambda_m + r_s^2 \lambda_s \right)} \pi^2 r \lambda_m \left(\frac{\frac{2\alpha_s}{\Delta_m} r_s^{\frac{\alpha_s}{\alpha_m}}}{\Delta_m} \alpha_s \lambda_m + r_s^2 \alpha_m \lambda_s \right)}{r_s \alpha_m}.
\end{aligned} \tag{17}$$

- *Case (B)*: $\|r\| \in \nu_-^+(r_s, \Delta_m, \alpha_s, \alpha_m)$ This case has a finite intersection area between the backhaul disc and the inner macro disc. Thus the void probabilities and so the density is calculated as follows.

$$f(r_s, r) = \frac{\partial \left(e^{-\lambda_s \pi r_s^2} e^{-\lambda_m \left(\pi (\Delta_m^{-1} r_s^{\alpha_s / \alpha_m})^2 + \pi r^2 - \text{lens}(M_1, M_2) \right)} \right)}{\partial r_s \partial r}, \tag{18}$$

where $\text{lens}(M_1, M_2)$ denotes the area of the lens formed between points M_1 and M_2 of Fig. 2a (part (B)) and is given as in [30].

- *Case (C)*: $\|r\| > \nu_+(r_s, \Delta_m, \alpha_s, \alpha_m)$ This case has the backhaul disc completely engulf the inner macro disc and the density is given as follows.

$$\begin{aligned}
f(r_s, r) &= \frac{\partial \left(e^{-\lambda_s \pi r_s^2} e^{\lambda_m \pi r^2} \right)}{\partial r_s \partial r} \\
&= 4\pi^2 \lambda_m \lambda_s r r_s e^{-\pi(\lambda_m r^2 + \lambda_s r_s^2)}.
\end{aligned} \tag{19}$$

- 2) $0 < \Delta_m < 1$: For this case the radii of the discs depicted in Fig. 2a change as $r_s / \Delta_m > r_s$.

Similar three cases are depicted in Fig. 2b.

- *Case (A)*: $0 < \|r\| < \mu_-(r_s, \Delta_m, \alpha_s, \alpha_m)$ This case is a zero probability case since it is already known that there is no M-BS within radius $\|r_s\|^{\alpha_s / \alpha_m} \Delta_m^{-1}$.
- *Case (B)*: $\|r\| \in \mu_-^+(r_s, \Delta_m, \alpha_s, \alpha_m)$ Equation (18) could directly be used to give this density function.
- *Case (C)*: $\|r\| \geq \mu_+(r_s, \Delta_m, \alpha_s, \alpha_m)$ This case is similar to the engulfment case as *Case (C)* for $\Delta_m \geq 1$. Hence, the third part of the density function of Equation (19) could directly be used.

APPENDIX B

SMALL CELL COVERAGE PROBABILITY

Coverage probability of a user, given it is associated to a small cell is derived here. The coverage probability is denoted by $\Pr(\text{SIR}_{us} > T_s, \text{SIR}_{sm} > T_b \mid \varepsilon_s)$.

$$\Pr(\text{SIR}_{us} > T_s, \text{SIR}_{sm} > T_b \mid \varepsilon_s) = \mathbb{E}_{r_s, r} \left[\underbrace{\Pr(\text{SIR}_{us} > T_s, \text{SIR}_{sm} > T_b \mid r_s, r)}_{P'_{u,s}(T_s, T_b)} \right] \quad (20)$$

where, r_s and r denote the points of Fig. 3 and are varied over a region so that the event ε_s of equation (5) is always true.

The inner probability term of equation (20) is derived below. In interest of better clarity, the representation of conditioning on points r_s and r is dropped in the following derivation.

$$\begin{aligned} P'_{u,s}(T_s, T_b) &= \Pr \left(\frac{P_s g_{or_s} \|r_s\|^{-\alpha_s}}{\sum_{z \in A_1^c} P_s g_{oz} \|z\|^{-\alpha_s} + \sum_{z \in A_2^c} P_m g_{oz} \|z\|^{-\alpha_m} + P_m g_{or_m} \|r_m\|^{-\alpha_m}} > T_s, \right. \\ &\quad \left. \frac{P_m g_{r_s r_m} \|r\|^{-\alpha_m}}{\sum_{z \in A_1^c} P_s g_{r_s z} \|z - r_s\|^{-\alpha_s} + \sum_{z \in A_2^c} P_m g_{r_s z} \|z - r_s\|^{-\alpha_m} + \beta P_s} > T_b \right) \\ &\stackrel{(a)}{=} \Pr(g_{or_s} > k_s \|r_s\|^{\alpha_s} I_1, g_{r_s r_m} > k_m \|r\|^{\alpha_m} I_2), \end{aligned}$$

where (a) results by taking $k_s = T_s/P_s$ and $k_m = T_b/P_m$ and I_1 and I_2 are short notations for interference terms in SIR_{us} and SIR_{sm} terms. Areas A_1 and A_2 are as defined in (8). Following from the result above,

$$\begin{aligned} P'_{u,s}(T_s, T_b) &= \mathbb{E}_{I_1, I_2} [\Pr(g_{or_s} > k_s \|r_s\|^{\alpha_s} I_1, g_{r_s r_m} > k_m \|r\|^{\alpha_m} I_2 \mid I_1, I_2)] \\ &\stackrel{(b)}{=} \mathbb{E}_{I_1, I_2} [\Pr(g_{or_s} > k_s \|r_s\|^{\alpha_s} I_1) \Pr(g_{r_s r_m} > k_m \|r\|^{\alpha_m} I_2) \mid I_1, I_2] \\ &\stackrel{(c)}{=} \mathbb{E}_{I_1, I_2} [e^{-k_s \|r_s\|^{\alpha_s} I_1} e^{-k_m \|r\|^{\alpha_m} I_2} \mid I_1, I_2] \\ &\stackrel{(d)}{=} \mathbb{E}_{g_{oz}, g_{r_s z}, \Phi_s} \left[\prod_{z \in A_1^c} e^{(-k_s \|r_s\|^{\alpha_s} P_s g_{oz} \|z\|^{-\alpha_s})} e^{(-k_m \|r\|^{\alpha_m} P_s g_{r_s z} \|z - r_s\|^{-\alpha_s})} \right] \\ &\quad \mathbb{E}_{g_{oz}, g_{or_m}, g_{r_s z}, \Phi_m} \left[\prod_{z \in A_2^c} e^{(-k_s \|r_s\|^{\alpha_s} P_m (g_{oz} \|z\|^{-\alpha_m} + g_{or_m} \|r_m\|^{-\alpha_m}))} e^{(-k_m \|r\|^{\alpha_m} P_m g_{r_s z} \|z - r_s\|^{-\alpha_m})} \right] \\ &\quad e^{(-k_m \|r\|^{\alpha_m} \beta P_s)}. \end{aligned}$$

Assumption of independently fading links gives result to (b). Result in (c) is based on the assumption of fading power being exponentially fading with unit mean. Expanding I_1 , I_2 and separating terms belonging to the independent processes Φ_m and Φ_s , the result is as given by (d). Simplifying further,

$$\begin{aligned}
P'_{u,s}(T_s, T_b) &\stackrel{(e)}{=} \mathbb{E}_{g_{oz}, g_{r_s z}, \Phi_s} \left[\prod_{z \in A_1^c} e^{(-k_s \|r_s\|^{\alpha_s} P_s g_{oz} \|z\|^{-\alpha_s})} e^{(-k_m \|r\|^{\alpha_m} P_s g_{r_s z} \|z-r_s\|^{-\alpha_s})} \right] \\
&\mathbb{E}_{g_{oz}, g_{r_s z}, \Phi_m} \left[\prod_{z \in A_2^c} e^{(-k_s \|r_s\|^{\alpha_s} P_m(g_{oz} \|z\|^{-\alpha_m})} e^{(-k_m \|r\|^{\alpha_m} P_m g_{r_s z} \|z-r_s\|^{-\alpha_m})} \right] \\
&\mathbb{E}_{g_{orm}} \left[e^{-k_s \|r_s\|^{\alpha_s} P_m g_{orm} \|r_m\|^{-\alpha_m}} \right] e^{(-k_m \|r\|^{\alpha_m} \beta P_s)} \\
&\stackrel{(f)}{=} \exp \left(-\lambda_s \int_{z \in A_1^c} 1 - \frac{1}{(1 + k_s \|r_s\|^{\alpha_s} P_s \|z\|^{-\alpha_s})(1 + k_m \|r\|^{\alpha_m} P_s \|z-r_s\|^{-\alpha_s})} dz \right) \\
&\exp \left(-\lambda_m \int_{z \in A_2^c} 1 - \frac{1}{(1 + k_s \|r_s\|^{\alpha_s} P_m \|z\|^{-\alpha_m})(1 + k_m \|r\|^{\alpha_m} P_m \|z-r_s\|^{-\alpha_m})} dz \right) \\
&e^{(-k_m \|r\|^{\alpha_m} \beta P_s)} \left(\frac{1}{1 + k_s \|r_s\|^{\alpha_s} P_m \|r_m\|^{-\alpha_m}} \right).
\end{aligned}$$

Result in (e) simply follows from (d) by separating terms that depend on either Φ_m or Φ_s and the ones that do not. The final step in (f) uses the probability generating functional [21] of a PPP and the result of the work in [29], as was used in (23). Plugging the result of (f) in (20) and substituting the expectation with the pdf $f(r_s, r)$ gives the result of (8).

APPENDIX C

M-BS COVERAGE PROBABILITY IN IBFD SETTING

The coverage probability under M-BS could be derived as shown below:

$$\begin{aligned}
\Pr(\text{SIR}_{um} > T_m, \varepsilon_m) &\stackrel{(a)}{=} \mathbb{E}_{r'_m, r_s} [\Pr(\text{SIR}_{um} > T_m \mid r'_m, r_s)] \\
&= \mathbb{E}_{r'_m, r_s} \left[\Pr \left(\underbrace{\frac{P_m g_{or'_m} r'^{-\alpha_m}}{\sum_{z \in \Phi_m \cap B(o, r'_m)^c} P_m g_{oz} \|z\|^{-\alpha_m} + \sum_{z \in \Phi_s \cap B(o, \Delta_s r_m^{\alpha_m/\alpha_s})^c} P_s g_{oz} \|z\|^{-\alpha_s}} > T_m \mid r'_m, r_s} \right) \right].
\end{aligned} \tag{21}$$

The result in (a) follows as r_s and r'_m are varied so that event ε_m is always true which is in accordance with the limits of integration in (10). Let the interference (denominator) term in (21) be denoted by $I(\Phi_m, \Phi_s)$, where Φ_x could be thought of as the process defining the entire characteristics of tier x . Therefore, $\Phi_m \triangleq \{\lambda_m, P_m, T_m, B_m\}$ and $\Phi_s \triangleq \{\lambda_s, P_s, T_s, B_s\}$. The term $F(\Phi_m, \Phi_s)$ is simplified as follows.

$$\begin{aligned} F(\Phi_m, \Phi_s) &= \Pr \left(\frac{P_m g_{or'_m} r'^{-\alpha_m}}{I(\Phi_m, \Phi_s)} > T_m \mid r'_m, r_s \right) \\ &\stackrel{(a)}{=} \mathbb{E}_{I(\Phi_m, \Phi_s)} \left[e^{-(T_m/P_m) r'^{\alpha_m} I(\Phi_m, \Phi_s)} \mid r'_m \right], \end{aligned} \quad (22)$$

where, (a) follows from $g_{or'_m}$ being a unit mean exponential random variable and $F(\Phi_m, \Phi_s)$ being independent of r_s . Continuing further,

$$\begin{aligned} F(\Phi_m, \Phi_s) &= \mathbb{E}_{I(\Phi_m, \Phi_s)} \left[e^{-T_m r'^{\alpha_m} \sum_{z \in \Phi_m \cap B(o, r'_m)^c} g_{oz} \|z\|^{-\alpha_m}} e^{-\frac{T_m P_s r'^{\alpha_m}}{P_m} \sum_{x \in \Phi_s \cap B(o, \Delta_s r'_m)^{c}} g_{ox} \|x\|^{-\alpha_s}} \mid r'_m \right] \\ &\stackrel{(b)}{=} \mathbb{E}_{g_{oz}, \Phi_m} \left[\prod_{z \in \Phi_m \cap B(o, r'_m)^c} e^{-T_m r'^{\alpha_m} g_{oz} \|z\|^{-\alpha_m}} \mid r'_m \right] \mathbb{E}_{g_{ox}, \Phi_s} \left[\prod_{x \in \Phi_s \cap B(o, \Delta_s r'_m)^{c}} e^{-\frac{T_m P_s r'^{\alpha_m}}{P_m} g_{ox} \|x\|^{-\alpha_s}} \mid r'_m \right] \\ &\stackrel{(c)}{=} e^{-\pi r'^2 \lambda_m T_m^{2/\alpha_m} \int_{T_m^{-2/\alpha_m}}^{\infty} \frac{1}{1+t^{\alpha_m}/2} dt} e^{-\pi r'^{2\alpha_m/\alpha_s} \lambda_s \left(\frac{P_s T_m}{P_m}\right)^{\frac{2}{\alpha_s}} \int_{\left(\frac{B_s}{B_m T_m}\right)^{\frac{2}{\alpha_s}}}^{\infty} \frac{1}{1+t^{\alpha_s}/2} dt}, \end{aligned} \quad (23)$$

where (b) follows from the independence of the processes Φ_m and Φ_s and the assumption of fading on links being independent. Finally, (c) follows from the single-tier coverage probability result in [29].

APPENDIX D

M-BS TO USER RATE

Rate under M-BS in the IBFD setting could be derived as follows:

$$\begin{aligned} \mathbb{E} [R_{um} \mid \text{SIR}_{um} > T_m] &= \mathbb{E} [\bar{\eta} \log(1 + \text{SIR}_{um}) \mid \text{SIR}_{um} > T_m] \\ &\stackrel{(a)}{=} \bar{\eta} \int_{t \geq 0} \Pr(\log(1 + \text{SIR}_{um}) > t \mid \text{SIR}_{um} > T_m) dt \\ &= \bar{\eta} \int_{t > 0} \Pr(\text{SIR}_{um} > 2^t - 1 \mid \text{SIR}_{um} > T_m) dt \\ &= \frac{\bar{\eta}}{\Pr(\text{SIR}_{um} > T_m)} \int_{t > 0} \Pr(\text{SIR}_{um} > \max(2^t - 1, T_m)) dt, \end{aligned} \quad (24)$$

where (a) follows from the fact that the rate R_{um} is a positive random variable.

APPENDIX E

M-BS TO P-BS TO USER RATE ($\min(R_{us}, R_{sm})$)

The net rate obtained from P-BS is a minimum over M-BS to P-BS (backhaul) and P-BS to user (access) rates. This is derived as follows:

$$\begin{aligned}
\mathbb{E}[\min(R_{us}, R_{sm}) \mid \text{SIR}_{us,sm} > T_{s,b}] &= \int_{t>0} \Pr(\min(R_{us}, R_{sm}) > t \mid \text{SIR}_{us,sm} > T_{s,b}) dt \\
&= \int_{t>0} \Pr(R_{us} > t, R_{sm} > t \mid \text{SIR}_{us,sm} > T_{s,b}) dt \\
&= \int_{t>0} \Pr\left(\log(1 + \text{SIR}_{us}) > t, \frac{\eta}{n} \log(1 + \text{SIR}_{sm}) > t \mid \text{SIR}_{us,sm} > T_{s,b}\right) dt \\
&= \int_{t>0} \Pr\left(\text{SIR}_{us} > 2^t - 1, \text{SIR}_{sm} > 2^{\frac{nt}{\eta}} - 1 \mid \text{SIR}_{us,sm} > T_{s,b}\right) dt \\
&= \frac{1}{\Pr(\text{SIR}_{us,sm} > T_{s,b})} \int_{t>0} \Pr\left(\text{SIR}_{us} > \max(2^t - 1, T_s), \text{SIR}_{sm} > \max(2^{\frac{nt}{\eta}} - 1, T_b)\right) dt.
\end{aligned} \tag{25}$$